IOSR Journal of Applied Physics (IOSR-JAP)
e-ISSN: 2278-4861.Volume 9, Issue 3 Ver. I (May. – June. 2017), PP 67-81
www.iosrjournals.org

Effects of the deformation orders β6 & β8 on the fusion parameters for spherical-deformed interacting pair

M. Ismail [1], Maher H. Wasfy [2], I.A.M. Abdul-Magead [1] and I. M. Kandil [2]
[1]*(Physics Department, Faculty of Science, Cairo University, Egypt)*
[2]*(Physics Department, Faculty of Science, Suez University, Egypt)*

Abstract : *We investigated the effect of the deformation orders β6 & β8 on the fusion barrier parameters (namely; Coulomb barrier* VB *and its radius* RB*), using two methods the double folded model (DFM) using M3Y Reid nucleon-nucleon (NN) interaction with the zero range exchange term and proximity approach (PROX) which is composed of proximity 2000DP for calculating the nuclear part and Denisov potential for Coulomb part. It was found that PROX shows some abnormalities in the effect of the deformation order β6 & β8 on orientation dependence of the fusion barrier parameters.*

Keywords: *Deformation order, fusion barrier parameter, double folded model, proximity approach and spherical deformed.*

I. Introduction

The static deformations of nuclei affect the fusion cross-section and other nuclear quantities. So the deformation in one or in both of the colliding nuclei enhances strongly the fusion cross section [2, 3, 5, 11, 26, and 27]. Besides the cross sections of various nuclear reactions, the production of super heavy nuclei are mainly controlled by the Coulomb barrier which is sensitive to nuclear deformations [3, 5]. The study of variation of the Coulomb barrier parameters with the orientation angles and deformation orders of deformed interacted nuclei is essentially important in describing reactions and decay processes [2, 5].

The interaction potential between two nuclei consists mainly of nuclear and Coulomb parts. The Coulomb and nuclear parts are calculated from six-dimensional integral in the frame work DFM [4, 5, 11, 14, 15, 17, 19, 21, and 29]. The proximity approach [3, 8, 24, and 28] was also used to calculate the nuclear interaction potential between two nuclei. It is based on the proximity theorem [8] which simplifies the interacting potential as a simple function of the product of a universal function, $\xi(x = S_{Min}/b)$ [3, 6, 8, 20, 23, 24, 25, 28], and the geometrical factor, R, and other quantities as surface energy coefficient, γ, and nuclear surface thickness, b. The universal function represents the dimensionless interacting potential, it depends on the surface minimum separation distance, S_{Min}. The geometrical factor represents the transformation Jacobean of the variable of the integral [8], which describe the geometry of the gap between the two interacting nuclei [7,8, 25]. It is based on the shapes and the relative orientation of the interacting nuclei. Due to the simplicity of the proximity approach, it is frequently used in calculating the nuclear potential between two interacting spherical nuclei [10]. Recently, the proximity theorem has been extended to drive the nuclear interaction for spherical–deformed and deformed–deformed nuclei [1, 2, 3, 11, 12, 14, 15, 16, 17, 21, and 25].

Many authors have investigated the effect of deformation orders on the fusion barrier parameters [1, 2, 3, 5, 6, 8, 9, 11, 12, 13, 14, 15, 16, 17, 19, 20, 21, 23, 25, 27]. Most authors have studied the effect of the deformation orders {β2, β3 & β4} on the fusion barrier parameter and fusion cross section [3, 12, 14, 16, 17, and 18]. Ismail [17] discussed the effect of deformation orders β3, β6 and β8, on the distribution of fusion barriers in orientation degrees of freedom in the frame work of the double folding model with the realistic M3Y NN interaction. In this paper we will assess the proximity approach in calculating the fusion barrier parameter for spherical-deformed interacting pair of nuclei, where the deformed nucleus has higher deformation orders, β6 and β8. In addition we will study effects of β6 and β8 on the fusion barrier, then a comparative study will be made between the proximity approach results and the DFM ones.

This paper is organized as follows: Section 2 includes the formulation of the proximity approach afterward that of the double folded model. Section 3 contains the results and discussion of the effect of deformation orders β6 and β8 on fusion barrier parameter. We end up the paper with summary and conclusion in Section 4.

II. Formulation

In the first place we will formulate the proximity potential (PROX) to calculate the nuclear potential. We use its definition as following, [3, 8, 7, 20, 23, 24, 25, 28]

$$V_N(R) = 4\pi\gamma\, b\, R\, \xi\left(\frac{S_{min}}{b}\right), \tag{1}$$

where R is the distance between the centers of mass of the interacting nuclei, γ is the surface energy coefficient, b the nuclear surface thickness, R is the geometrical factor, ξ is the universal function and Smin is the minimum distance between the surfaces of the interacting pair of nuclei. The surface energy coefficient [14,15] can be calculated by,

$$\gamma = \frac{1}{4\pi r_o^2}\left\{18.63 - Q\,\frac{(t_1^2+t_2^2)}{2\, r_o^2}\right\}, \tag{2}$$

where Q is the neutron skin stiffness coefficient and ti is the neutron skin of the nucleus,[14,15]

$$t_i = \frac{3}{2}\, r_o \left[\frac{J\, I_i + \frac{b_1 Z_i}{12\sqrt[3]{A_i}}}{Q + \frac{9J}{4\sqrt[3]{A_i}}}\right] \tag{3}$$

where J is the nuclear symmetry energy coefficient, $I_i = \frac{(N_i - Z_i)}{A_i}$, b1 = 0.757895 MeV and r0 = 1.14 fm [14,15].

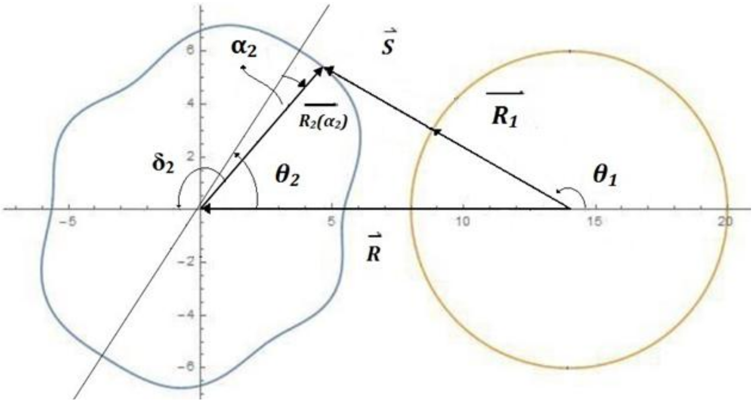

Figure 1 Schematic configuration of the spherical and the axially symmetric deformed nuclei. The symmetric axis of the deformed nuclei is in the direction of θ2

To calculating the minimum distance, Smin, we need to minimize the surfaces separation distance, S, by making use of Fig. (1) where, we will find that [14].

$$\bar{S} + \bar{R}_1 = \bar{R} + \bar{R}_2(\alpha_2), \tag{4}$$

$$S = \left(R^2 + R_2^2(\alpha_2) + 2\, R\, R_2(\alpha_2)\cos\delta_2\right)^{1/2} - R_{01}, \tag{5}$$

Where the angle α2 can be expressed in terms of δ2 as α2 = δ2 + θ2 − π.
While the universal function ξ(x) is given as [7, 14, 15]

$$\xi(x) = \begin{cases} -0.1353 + \sum_{n=0}^{5} \frac{c_n}{n}\left(2.5 - \frac{x}{b}\right) & ; 0 \le x \le 2.5 \\ -0.09551\, Exp\left[\frac{2.75 - \frac{x}{b}}{0.7176}\right] & ; x \ge 2.5 \end{cases} \tag{6}$$

where C0 = − 0.1886, C1 = − 0.2628, C2 = − 0.15216, C3 = − 0.04562, C4 = 0.069136 & C5 = − 0.011454 [6, 11, 15, 21, 25, 27]. The geometrical factor is given by the following relation,

$$\bar{R} = \left(\frac{1}{R_{11}}\frac{1}{R_{12}} + \frac{1}{R_{21}}\frac{1}{R_{22}} + \frac{1}{R_{11}}\frac{1}{R_{22}} + \frac{1}{R_{21}}\frac{1}{R_{12}}\right)^{-\frac{1}{2}} \tag{7}$$

where R11, R12, R21 & R22 are the principal radii of curvature of the gap between the two interacting nuclei [6, 11, 15, 21, 25, 27] and are calculated using the relations below [4, 7, 11, 15, 21, 22, 25, 27],

$$R_{i1}(\alpha_i) = \frac{\left[R_i^2(\alpha_i) + R_i'^2(\alpha_i)\right]^{3/2}}{2\,R_i^2(\alpha_i) + 2\,R_i'^2(\alpha_i) - R_i(\alpha_i)\,R_i''(\alpha_i)} \qquad ;i = 1\,,2 \tag{8}$$

$$R_{i1}(\alpha_i) = \frac{R_i(\alpha_i)\,\sin\alpha_i}{\cos\left[(-1)^{i-1}\frac{\pi}{2} - \theta_i\right]} \qquad ;i = 1\,,2 \tag{9}$$

As known that the radius of a deformed nucleus of an axially symmetric deformation can be written as [4, 7, 11, 15, 21, 22, 25, 27],

$$R_i(\alpha_i) = R_{0i}\left(1 + \sum_{l\,\epsilon\,\{2,3,4,6,8\}} \beta_{i\,l}\,Y_l^0(\alpha_i\,,0)\right) \qquad ;i = 1{,}2 \tag{10}$$

R0i is the matter radius, βi, l is the deformation parameter of order l, Yl0(θ, φ) is the spherical harmonic of order l. In PROX the matter radius [14, 15] is calculated as,

$$R_{0i} = c_i + \frac{N_i}{A_i} t_i \qquad ;\mathrm{i} = 1, 2 \tag{11}$$

Where ci denotes the half-density radii of the nuclear charge distribution [14, 15],

$$c_i = R_{00i}\left(1 - \frac{7}{2}\left(\frac{b}{R_{00i}}\right)^2 - \frac{49}{8}\left(\frac{b}{R_{00i}}\right)^4 + \cdots\right) \qquad ;\mathrm{i} = 1, 2 \tag{12}$$

$$R_{00i} = 1.2332\ \sqrt[3]{A_i}\ \left(1 + \frac{2.348443}{A_i} - 0.151541\ I_i\right) \quad fm\,;\mathrm{i} = 1, 2 \tag{13}$$

The Coulomb part of the interaction between spherical-deformed pair of nuclei using the relation deduced by Denisov [14, 15, 27].

$$V_c(R,\theta_2) = \frac{Z_1\,Z_2\,e^2}{R}\left[1 + \sum_{l\geq 2}\{f_{1\,l}(R,\theta_2,R_{02})\,\beta_{2\,l}\} + f_2\,(R,\theta_2,R_{02})\,\beta_{2\,2}^{\,2}\right] \tag{14}$$

where

$$f_{1\,l}(R,\theta_2,R_{02}) = \frac{3\,R_{02}^l}{(2\,l+1\,)\,R^l}\ Y_l^0(\theta_2,0)$$

$$f_2\,(R,\theta_2,R_{02}) = \frac{6\,\sqrt{5}\,R_{02}^2}{35\,\sqrt{\pi}\,R^2}\ Y_2^0(\theta_2,0) + \frac{3\,R_{02}^4}{7\,\sqrt{\pi}\,R^4}\ Y_4^0(\theta_2,0)$$

We will then go on to present the nuclear potential in DFM, which is given by [4, 5, 11, 14, 15, 17, 19, 21, 29];

$$U_{DFM}(\bar{R}) = \int dr_1^3 \int dr_2^3\ \rho_1(\vec{r_1})\,V_{NN}\left(S = \left|\bar{R} + \vec{r1} - \vec{r2}\right|\right)\rho_2(\vec{r_2}) \tag{15}$$

where ρ1(⟶r1) & ρ2(⟶r2) are the density functions of the projectile and the target nuclei respectively, VNN(S) is the NN interaction potential, and ⟶R is the relative position vector of the centers of mass of the interacting pair of nuclei. To simplify calculation of the six dimensional integral (eq. 15) of the DFM, we will write VNN(S) in terms of its Fourier transform as [4, 11, 14, 15, 17, 19, 21],

$$V_{NN}(\bar{S}) = \int dk^3\ \tilde{V}_{NN}(k)\,e^{-i\,\bar{k}.\bar{S}} \tag{16}$$

We used the M3Y-Ried NN interaction with zero-range approximation for the exchange contribution [11, 14, 15, 17, 21, 29],

$$V_{NN}(\bar{S}) = 7999\ \frac{e^{-4\,s}}{4\,s} - 2134\ \frac{e^{-2.5\,s}}{2.5\,s} - 262\ \delta(\vec{S}) \tag{17}$$

As for the Coulomb potential, it is used as [11, 14, 15, 17, 21, 29],

$$V_{NN}^{Coulomb}(\bar{S}) = \frac{e^2}{s} \tag{18}$$

Furthermore, we used the multi pole expansion [19] for density distributions for separating the radial part from the angular dependent part for the density of the deformed nucleus. We finally reach after calculations to:

$$U_{DFM}(\vec{R}) = 8 \sum_{l} \int dk\ k^2\, Y_l^0(\Omega_T)\ \tilde{V}_{NN}(k)\, j_l(kR)\, A_1^0(k)\, A_2^l(k) \tag{19}$$

where A2l(k) and A10(k) are the form factors for target and projectile nuclei respectively. The form factors are given as

$$A_2^l(k) = \int dr_2\ r_2^2\, j_l(k r_2)\, \rho_2^l(r_2), \tag{20}$$

$$A_1^0(k) = \int dr_1\ r_1^2\, j_0(k r_1)\, \rho_1(r_1), \tag{21}$$

$$\rho_2^l(r_2) = \int d\hat{r}_2\ \rho_2(r_2, \theta_2, \varphi_2)\ Y_l^{*m}(\hat{r}_2). \tag{22}$$

The Fermi shape is employed to describe both projectile and target densities,

$$\rho_1(r_1, \theta_1, \varphi_1) = \frac{\rho_1^0}{(1 + Exp[(r - R_{01})/a])}$$

$$\rho_2(r_2, \theta_2, \varphi_2) = \frac{\rho_2^0}{\left(1 + Exp\left[\left(r - R_{02}(\alpha_2)\right)/a\right]\right)}$$

where ρ_1^0 & ρ_2^0 is the densities normalization constant, a is the diffuseness parameter which is equal to 0.5 fm [13]. As the matter radius [9] used here in DFM is given by,

$$R_{0i}=1.31\, A_i^{1/3} - 0.84 \qquad ; i = 1, 2 \tag{23}$$

III. Results and Discussion

In this section we will study the effect of the deformation orders β_6 & β_8 on the fusion barrier parameters computed spherical-deformed interacting nuclei by two methods, PROX and DFM. So, we will consider the nucleus Fe^{65} as a spherical projectile and the deformed nuclei {F^{45}, Si^{64}, Ba^{159} & U^{228} } as a target nucleus of orientation angle θ_2 and various deformation orders { β_2 , β_3 , β_4 & β_6 }. Values of { β_2 , β_3 , β_4 & β_6 } for all target nuclei are listed in Table1. For this study we will use the quantity defined as the relative variation in the radius of Coulomb barrier and it is given by (eq.24).

$$R_r = \frac{R_B(\text{With the studied deformation order}) - R_B(\text{Without the studied deformation order})}{R_B(\text{Without the studied deformation order})} \times 100\% \tag{24}$$

Table 1 The target nuclei and their deformation order parameters values [22].

Ele Element symbol ment	β_2	β_4	β_6
F^{45}	0.320	0.195	0.115
Si^{64}	-0.256	0.153	-0.097
Ba^{159}	0.273	0.02	-0.04
U^{228}	0.186	0.126	0.035

In first place we will discuss the effect of the deformation order β6 on the fusion barrier parameters, afterward the deformation order β_8 effects. Indeed different target nuclei are used in our study, in order to investigate different behaviors that give us more information about the effect of the higher order deformation parameters.

1 Deformation order β_6

In this subsection we study the deformation order β_6 effect on the radius of Coulomb barrier and are interested to know how much the consistency between the proximity and DFM results. Initially, as an illustrative example, as can be seen from Fig.2 the effect of deformation order β_6 with values $\beta_6 = \pm\, 0.3$ when added to a spherical nucleus surface of a nucleus has a matter radius $R_0 = 5\ fm$.

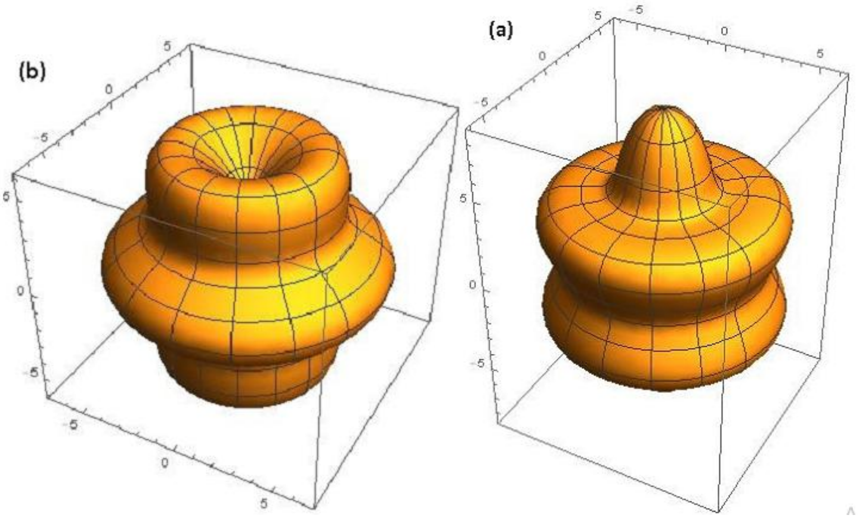

Figure 2 (a) The nucleus shape having only the deformation order $\beta_6 = 0.3$, the mater radius is 5 fm and other deformation orders have zero value. (b) The same as (a) except for the deformation order $\beta_6 = -0.3$.

Fig.3 presents the effect of the deformation order β_6 on the relative variation calculated using (eq.24) in the radius of Coulomb barrier as a function of the orientation angle θ_2 . This relative variation is evaluated using both methods of DFM and PROX for the reaction systems $Fe^{65}+F^{45}$, $Fe^{65}+Si^{64}$, $Fe^{65}+Ba^{159}$ & $Fe^{65}+U^{228}$. The results of DFM show smooth dependence of the relative variation in R_B on β_6 as seen in Figs.3 a and c. In contrast PROX presents abnormal behavior of the effect of β_6 on the relative variation in R_B as shown in Figs.3 b and d . These abnormalities appear as the deformed nucleus gets lighter or as the value of the order of deformation gets higher. A deep minimum occurs for the two reactions $Fe^{65}+F^{45}$ & $Fe^{65}+Si^{64}$ at orientation angles 40^o and 62.5^o respectively in Fig.3 b. Inspecting in the values of deformation parameters of these deformed nuclei, we conclude that the reason of abnormal behavior of R_r is that the deformation order β_6 produces concave regions in the nucleus surface and the surface becomes more irregular. These surface irregularities contradict the assumption of gently-curved surface based on in PROX.

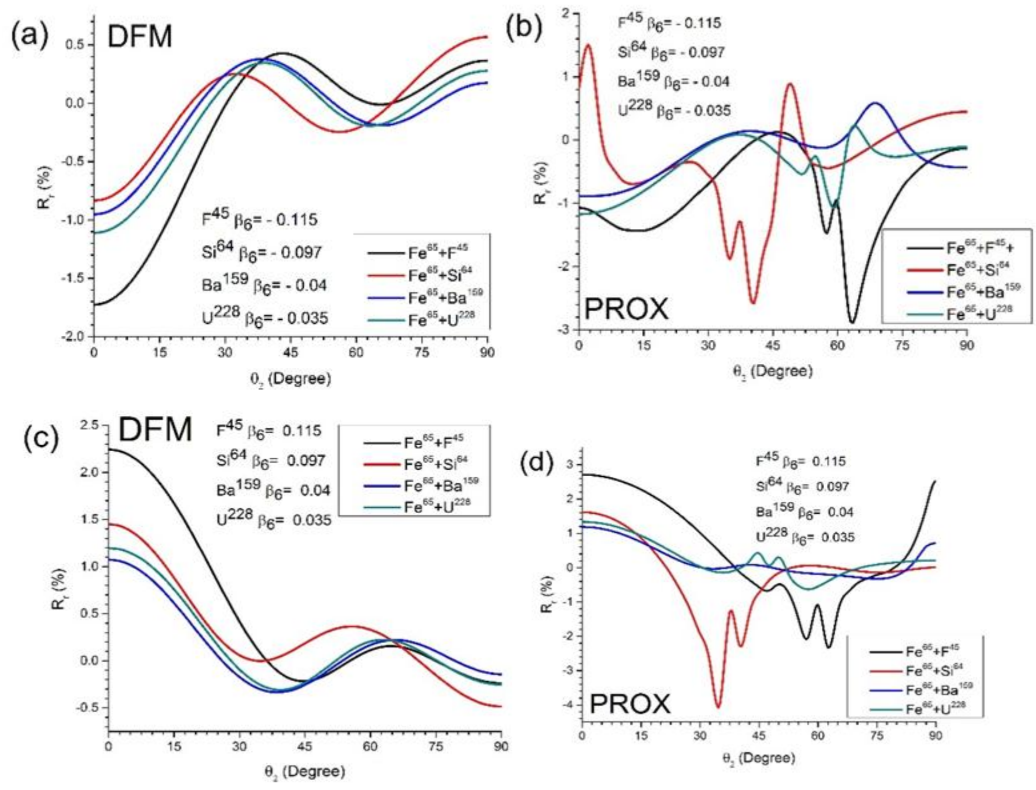

Figure 3 (a) The relative variation of the radius of the Coulomb barrier, R_r, plotted as a function of the orientation angle θ_2 for $Fe^{65} + F^{45}$, $Fe^{65} + Si^{64}$, $Fe^{65} + Ba^{159}$ & $Fe^{65} + U^{228}$ interaction systems, at deformation parameters written on Table1 using the negative value of β_6, in the frame wok DFM. (b) The same as (a) except for using PROX.(c) The same as (a) except for β_6 have the positive value. (d)The same as (b) except for β_6 have the positive value.

Fig.4 shows the orientation dependence of the radius of Coulomb barrier R_B for the reaction systems $Fe^{65} + F^{45}$; $Fe^{65} + Si^{64}$; $Fe^{65} + Ba^{159}$ & $Fe^{65} + U^{228}$; at deformation order $\beta_6 = \pm 0.115;\ 0.097;\ 0.04\ \&\ 0.035$ for the deformed target F^{45} , Si^{64} , Ba^{159} & U^{228} respectively, using DFM and PROX. According to the comparison between the DFM results and the proximity ones as shown in Fig.4, the effect of β_6 on R_B using PROX behaves similar to that behavior of DFM for heavy target nuclei U^{228} and Ba^{159}, especially for angles less than 55^o. On the contrary for light nuclei Si^{64} and F^{45}, PROX gives abnormal behaviors of the effect of the deformation parameter β_6 on the fusion barrier parameter R_B. This is due to the increases of the surface irregularities and concave regions on lighter nuclei.

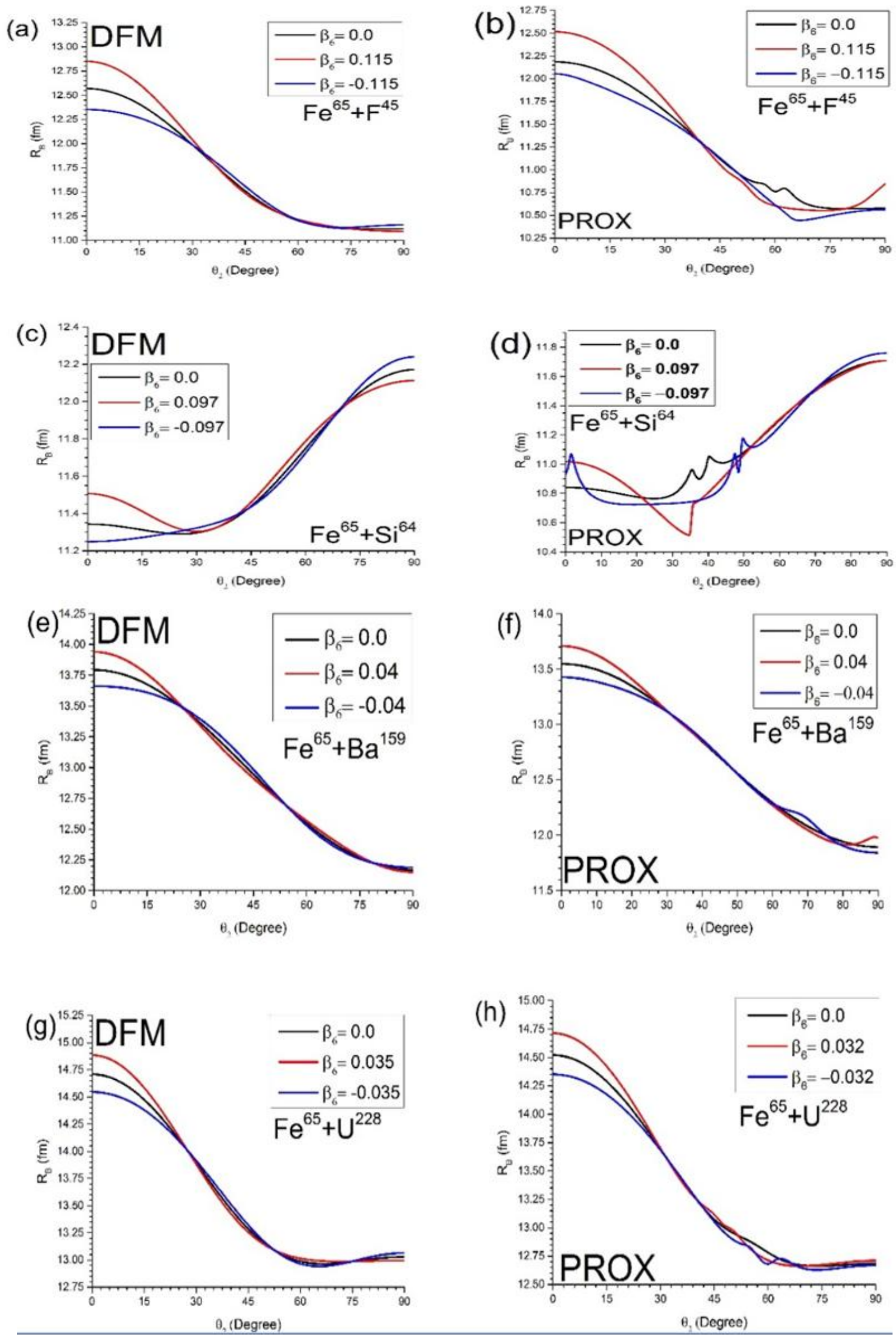

Figure 4 The radius of the Coulomb barrier, RB, plotted as a function of the orientation angle θ_2 for $Fe^{65} + F^{45}$ interaction, in the frame work of DFM in Fig. a and proximity in Fig. b. Figures c & d are the same

as a & b except for the reaction $Fe^{65} + Si^{64}$. Figures e & f are the same as a & b except for the reaction $Fe^{65} + Ba^{159}$. Figures g & h are the same as a & b except for the reaction $Fe^{65} + U^{228}$. We employed the deformation parameters of the deformed nuclei written on Table 1 using negative, positive and zero value of β_6.

Table 2 The values of the fusion barrier parameters R_B and V_B and their relative variation R_r and V_r for $Fe^{65} + F^{45}$ & $Fe^{65} + Si^{64}$ interaction systems, using DFM and PROX.

Reaction	θ_2	R_B	R_r	V_B	V_r	R_B	R_r	V_B	V_r	β_6
	(Deg)	*(fm)*		*(Mev)*		*(fm)*		*(Mev)*		
		DFM	DFM	DFM	DFM	PROX	PROX	PROX	PROX	
$Fe^{65}+F^{45}$	0	12.85	2.24	25.24	-2.06	12.52	2.71	25.70	-2.52	0.115
	10	12.74	1.98	25.42	-1.82	12.43	2.52	25.86	-2.35	
	20	12.45	1.28	25.96	-1.14	12.17	1.94	26.33	-1.83	
	30	12.04	0.42	26.72	-0.29	11.77	1.02	27.10	-1.00	
	40	11.64	-0.15	27.47	0.23	11.28	-0.12	28.08	0.04	
	50	11.36	-0.15	27.97	0.14	10.90	-0.48	28.97	0.61	
	60	11.22	0.11	28.17	-0.18	10.60	-1.08	29.59	1.36	
	70	11.14	0.11	28.23	-0.19	10.56	-0.45	29.63	0.41	
	80	11.10	-0.12	28.26	0.06	10.58	0.05	29.53	-0.02	
	90	11.09	-0.24	28.26	0.20	10.85	2.53	28.84	-2.26	
	0	12.35	-1.73	26.21	1.70	12.06	-1.07	26.63	1.00	-0.115
	10	12.32	-1.45	26.26	1.41	11.95	-1.41	26.84	1.34	
	20	12.20	-0.77	26.44	0.69	11.78	-1.29	27.16	1.24	
	30	11.99	-0.02	26.78	-0.07	11.57	-0.69	27.55	0.65	
	40	11.71	0.40	27.28	-0.46	11.29	-0.04	28.08	0.04	
	50	11.42	0.32	27.84	-0.32	10.96	0.02	28.77	-0.06	
	60	11.21	0.04	28.22	0.02	10.61	-1.00	29.55	1.22	
	70	11.13	0.02	28.29	0.04	10.46	-1.37	29.89	1.27	
	80	11.14	0.24	28.18	-0.21	10.53	-0.39	29.64	0.37	
	90	11.16	0.37	28.11	-0.35	10.56	-0.13	29.54	0.12	
$Fe^{65}+Si^{64}$	0	11.51	1.45	42.19	-1.41	11.34	1.62	42.80	-1.62	0.097
	10	11.46	1.18	42.39	-1.14	11.33	1.29	42.88	-1.32	
	20	11.36	0.55	42.87	-0.49	11.30	0.22	43.08	-0.36	
	30	11.30	0.06	43.24	0.04	11.30	-1.93	43.22	1.67	
	40	11.37	0.06	43.13	0.01	11.37	-2.27	43.13	2.07	
	50	11.56	0.31	42.58	-0.30	11.53	-0.16	42.71	0.10	
	60	11.79	0.33	41.94	-0.36	11.75	0.05	42.09	-0.06	
	70	11.97	0.04	41.45	-0.08	11.96	-0.09	41.48	0.09	
	80	12.08	-0.33	41.17	0.30	12.12	-0.11	41.05	0.11	
	90	12.11	-0.49	41.09	0.46	12.17	0.01	40.90	-0.01	
	0	11.25	-0.83	43.18	0.88	11.02	0.84	43.95	-0.82	-0.097
	10	11.26	-0.60	43.15	0.62	10.96	-0.63	44.18	0.60	
	20	11.29	-0.10	43.10	0.06	10.80	-0.48	44.84	0.40	
	30	11.32	0.24	43.09	-0.31	10.58	-0.55	45.81	0.41	
	40	11.38	0.13	43.04	-0.19	10.81	-2.56	45.08	2.40	
	50	11.51	-0.17	42.78	0.17	11.06	0.75	44.23	-0.40	
	60	11.72	-0.22	42.20	0.25	11.31	-0.40	43.47	0.37	
	70	11.97	0.07	41.47	-0.04	11.50	-0.01	42.90	-0.01	
	80	12.17	0.42	40.89	-0.40	11.64	0.33	42.49	-0.33	
	90	12.24	0.57	40.67	-0.54	11.71	0.45	42.29	-0.44	

Table 3 The values of the fusion barrier parameters R_B and V_B and their relative variation R_r and V_r for $Fe^{65} + Ba^{159}$ & $Fe^{65} + U^{228}$ interaction systems, using DFM and PROX.

Reaction	θ_2	R_B	R_r	V_B	V_r	R_B	R_r	V_B	V_r	β_6
	(Deg)	*(fm)*		*(Mev)*		*(fm)*		*(Mev)*		
		DFM	DFM	DFM	DFM	PROX	PROX	PROX	PROX	
$Fe^{65}+Ba^{159}$	0	13.94	1.07	145.52	-1.06	13.71	1.19	147.40	-1.26	0.04
	10	13.86	0.86	146.22	-0.85	13.63	0.98	148.11	-1.05	
	20	13.64	0.33	148.11	-0.32	13.41	0.47	150.05	-0.51	
	30	13.34	-0.17	150.58	0.19	13.12	0.01	152.64	0.02	
	40	13.05	-0.33	152.89	0.34	12.85	0.06	154.96	0.08	
	50	12.79	-0.11	154.73	0.11	12.55	-0.04	157.37	0.09	
	60	12.57	0.17	156.30	-0.19	12.27	-0.18	159.59	0.06	
	70	12.36	0.19	157.87	-0.21	12.05	-0.28	161.48	0.08	
	80	12.21	-0.01	159.25	0.01	11.92	-0.22	162.85	0.17	
	90	12.15	-0.14	159.83	0.16	11.98	0.71	162.27	-0.45	
	0	13.66	-0.95	148.52	0.98	13.43	-0.89	150.78	1.01	-0.04

	10	13.64	-0.73	148.56	0.74	13.39	-0.82	151.01	0.89	
	20	13.56	-0.22	148.89	0.21	13.29	-0.47	151.51	0.46	
	30	13.40	0.24	149.90	-0.26	13.12	-0.04	152.54	-0.04	
	40	13.14	0.37	151.79	-0.38	12.87	0.14	154.43	-0.26	
	50	12.82	0.15	154.34	-0.15	12.56	-0.02	157.08	-0.09	
	60	12.53	-0.13	156.83	0.15	12.29	-0.05	159.65	0.10	
	70	12.32	-0.16	158.48	0.17	12.15	0.55	160.80	-0.34	
	80	12.22	0.04	159.14	-0.05	11.91	-0.31	162.90	0.20	
	90	12.19	0.18	159.27	-0.19	11.84	-0.43	163.32	0.19	
$Fe^{65}+U^{228}$	0	14.89	1.20	223.91	-1.12	14.72	1.33	224.46	-1.38	0.035
	10	14.75	0.99	225.62	-0.94	14.58	1.15	226.19	-1.21	
	20	14.38	0.47	230.49	-0.44	14.21	0.64	231.16	-0.71	
	30	13.88	-0.09	237.24	0.12	13.70	0.03	238.52	-0.06	
	40	13.42	-0.31	243.50	0.33	13.25	-0.02	245.79	0.22	
	50	13.13	-0.07	247.08	0.06	13.00	0.31	249.67	-0.12	
	60	13.01	0.20	247.85	-0.23	12.71	-0.55	252.55	0.20	
	70	12.99	0.14	247.31	-0.16	12.66	-0.03	252.21	-0.09	
	80	12.99	-0.12	246.67	0.10	12.69	0.15	251.35	0.01	
	90	13.00	-0.25	246.43	0.24	12.71	0.21	250.95	0.07	
	0	14.55	-1.11	228.91	1.08	14.35	-1.17	230.56	1.30	-0.035
	10	14.47	-0.90	229.76	0.87	14.27	-1.00	231.47	1.10	
	20	14.26	-0.37	232.31	0.35	14.04	-0.56	234.21	0.60	
	30	13.92	0.16	236.51	-0.18	13.68	-0.07	238.72	0.02	
	40	13.51	0.34	241.82	-0.36	13.26	0.06	244.62	-0.26	
	50	13.16	0.11	246.67	-0.11	12.90	-0.46	250.37	0.16	
	60	12.96	-0.17	248.89	0.19	12.66	-0.97	254.11	0.82	
	70	12.95	-0.11	248.03	0.13	12.64	-0.22	252.97	0.21	
	80	13.03	0.15	246.08	-0.14	12.65	-0.20	251.27	-0.02	
	90	13.07	0.28	245.17	-0.27	12.67	-0.11	250.38	-0.16	

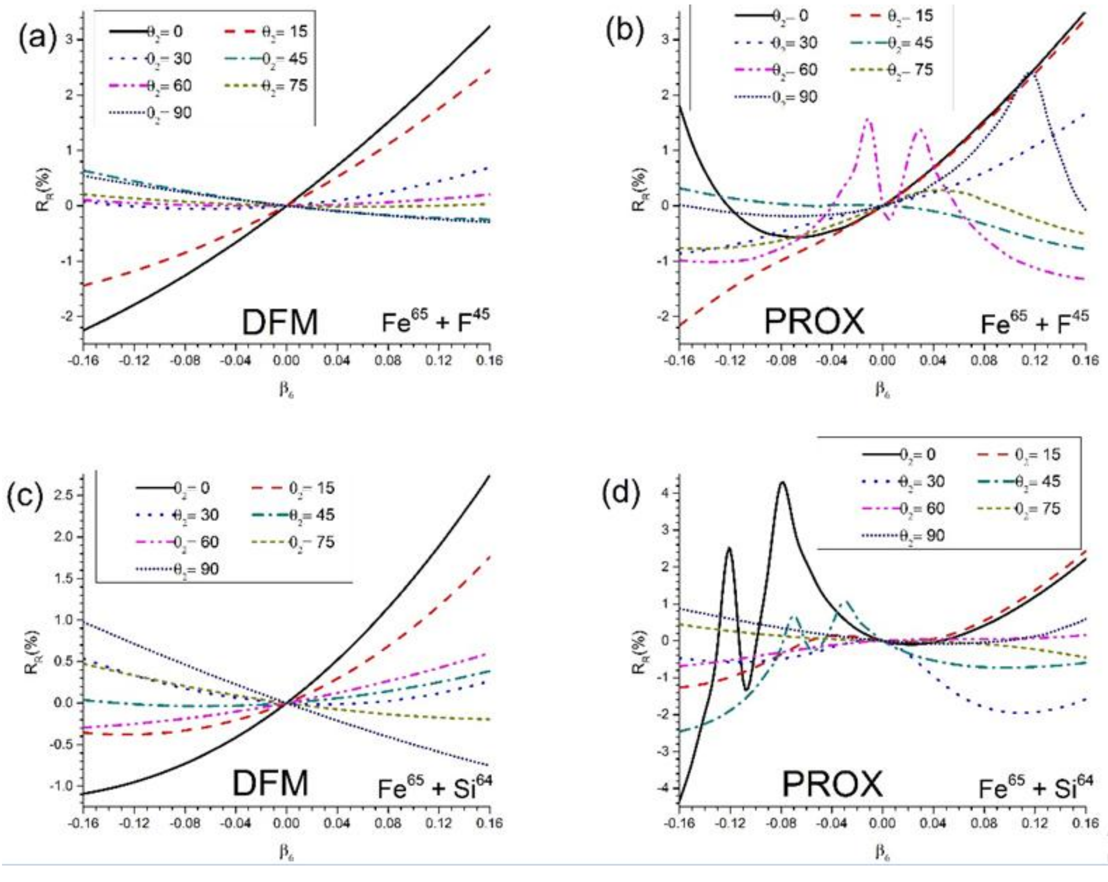

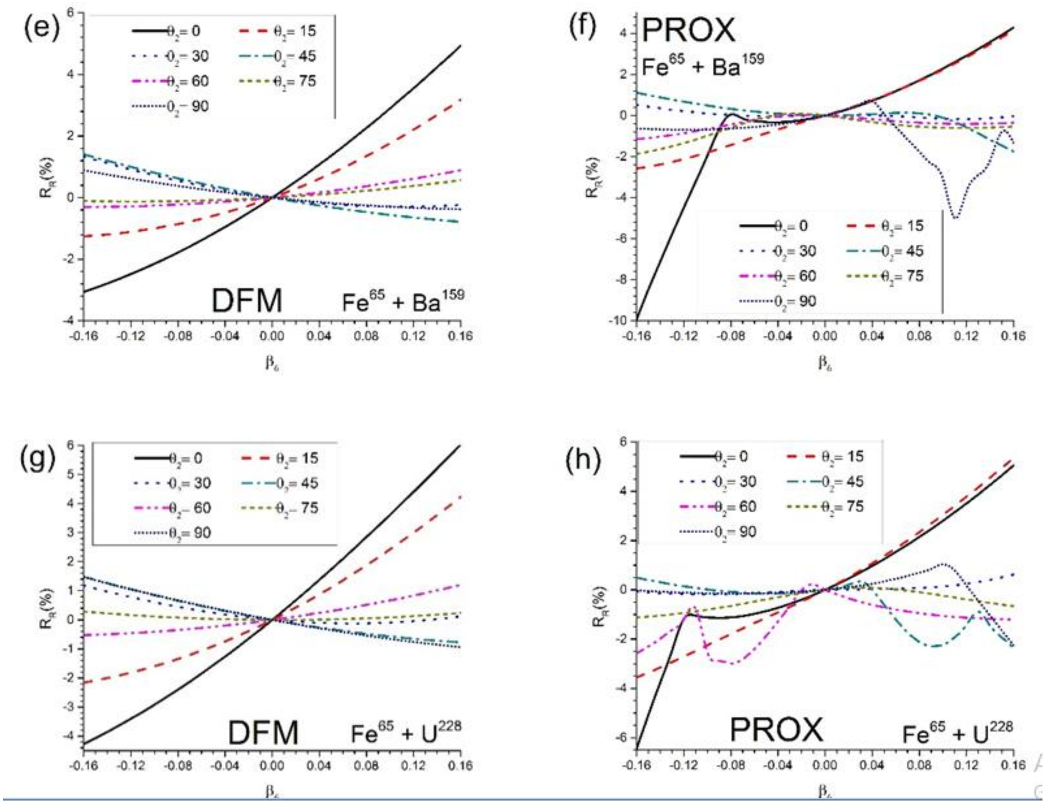

Figure 5 (a) The radius of the Coulomb barrier, R_r, plotted as a function of the deformation order β_6 for $Fe^{65} + F^{45}$ interaction at its data in Table1 in the frame work DFM. (b) The same as (a) except for using PROX. (c) The same as (a) except for $Fe^{65} + Si^{64}$ interaction. (d) The same as (b) except for $Fe^{65} + Si^{64}$ interaction. (e) The same as (a) except for $Fe^{65} + Ba^{159}$ interaction. (f) The same as (b) except for $Fe^{65} + Ba^{159}$ interaction.(g) The same as (a) except for $Fe^{65} + U^{228}$ interaction. (h) The same as (b) except for $Fe^{65} + U^{228}$ interaction.

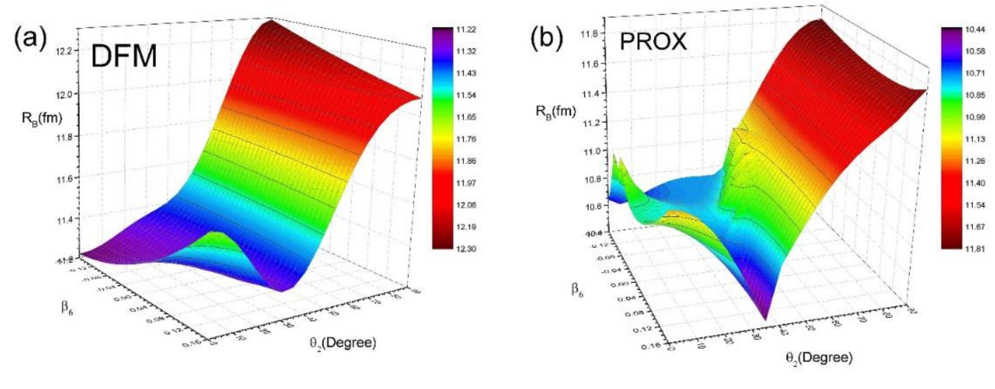

Figure 6 (a) The radius of the Coulomb barrier, R_B, plotted as a function of the orientation angle θ_2 and the deformation order β_6 for $Fe^{65} + Si^{64}$ interaction, using DFM calculation method. (b) The same as (a) except for using PROX calculation method.

As shown Fig.5 presents dependence of the relative variation of the radius of Coulomb barrier R_r on the deformation order β_6 at different orientation angles of the deformed target nucleus. The relative variation is calculated using DFM and PROX for $Fe^{65}+F^{45}$, $Fe^{65}+Si^{64}$, $Fe^{65}+Ba^{159}$ & $Fe^{65}+U^{228}$ interacting systems. It is obvious in Fig.5 that PROX shows non smooth and non-physical behaviors for the effect of β_6 on R_r compared to those resulted from DFM for some orientations. For example PROX produces strong dependence for R_r on β_6 when it becomes more negative at the orientation angle $\theta_2 = 0^o$ for all above reaction systems. In addition Fig.5 for the system $Fe^{65}+F^{45}$ shows that nonphysical behavior at $\theta_2 = 60^o$ for small β_6 values and at $\theta_2 = 30^o$ at more positive β_6 value. Fig.5 d shows also non smooth behavior at $\theta_2 = 45^o$. Moreover there exists abnormal behavior in Fig.5 f at $\theta_2 = 90^o$ as β_6 becomes more positive for the system $Fe^{65}+Ba^{159}$

and in Fig.5 h at $\theta_2 = 60^o$ for negative β_6 and $\theta_2 = 45^o$ for positive β_6 for the reaction $Fe^{65} + U^{228}$. Fig.6 ensures the non-consistency between the DFM results and PROX ones in three dimensional space when the radius of Coulomb barrier is plotted versus both deformation order β_6 and the orientation angle of symmetry axis of the deformed nucleus for the reaction $Fe^{65} + Si^{64}$.

Tab.2 shows quantitative behaviors of the fusion barrier parameters R_B and V_B and their relative variation R_r and V_r for $Fe^{65} + F^{45}$ and $Fe^{65} + Si^{64}$ interaction systems, using DFM and PROX for orientation angles from 0^o to 90^o at the positive and negative values of β_6 of the deformed target nuclei. Tab.3 is the same as Tab.2 except for the reaction systems $Fe^{65} + Ba^{159}$ and $Fe^{65} + U^{228}$. It is obvious that Tables 2-3 ensure and enhance the failure of PROX to reproduce smooth and Physical behaviors of dependence of the fusion barrier on the symmetry axis orientation and the deformation order β_6 of the target nucleus. For instance from Tab.3 for U^{228} at $\theta_2 = 90^o$ PROX produces larger value for the fusion barrier height V_B than its value from DFM by the difference 5.21 MeV. This larger difference in V_B is effective in calculating the fusion cross sections.

2 Deformation order β_8

In this subsection we study the effect of the deformation order β_8 on the radius of Coulomb barrier R_B. In this study we are also interested to know how much the consistency between the proximity and DFM results.

Fig.7 presents the effect of the deformation order β_8 on the relative variation calculated using (eq.24) in the radius of Coulomb barrier as a function of the orientation angle θ_2. This relative variation is evaluated using both methods of DFM and PROX for the reaction systems $Fe^{65} + F^{45}$, $Fe^{65} + Si^{64}$, $Fe^{65} + Ba^{159}$ & $Fe^{65} + U^{228}$. The results of DFM show smooth dependence of the relative variation in R_B on β_8 as seen in Figs.7 a & c . In contrast PROX presents abnormal behavior of the effect of β_8 on the relative variation in R_B as shown in Figs.7 b and d. Inspecting the reason of the non-physical behaviors introduced by PROX, we reached to the reason of the non-physical behaviors is that the deformation order β_8 produces also more concave regions on the deformed nucleus surface whuch contradict the assumption of gently-curved surface based in PROX.

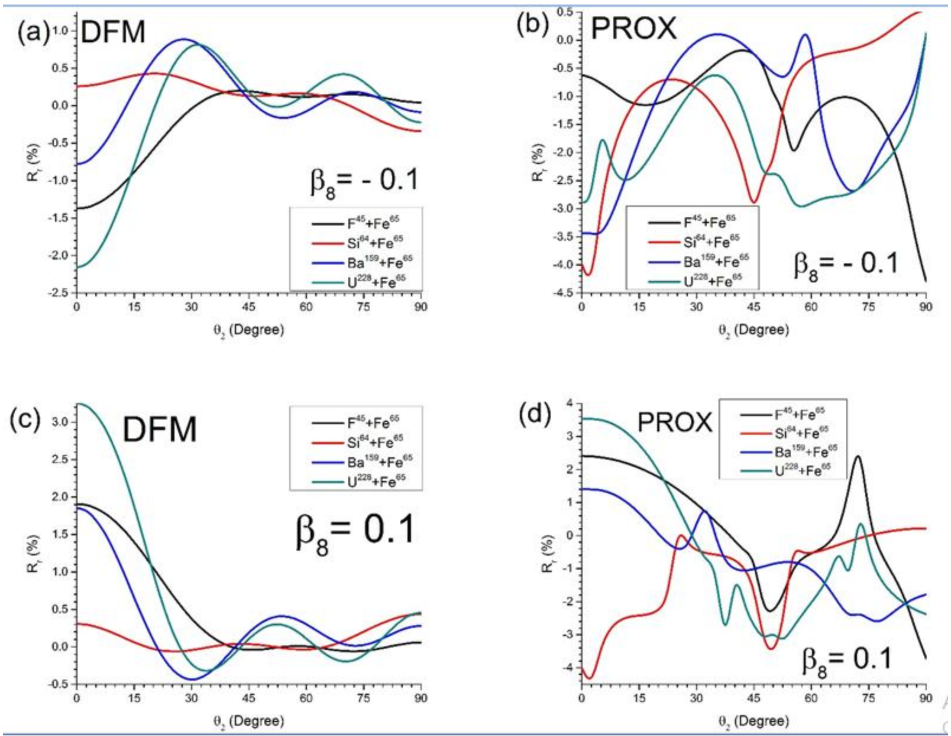

Figure 7 (a) The relative variation of the radius of the Coulomb barrier, R_r, plotted as a function of the orientation angle θ_2 for $Fe^{65} + F^{45}$, $Fe^{65} + Si^{64}$, $Fe^{65} + Ba^{159}$ & $Fe^{65} + U^{228}$ interaction systems, at deformation parameters written on Table1 using the negative value of β_8, in the frame wok DFM. (b) The same as (a) except for using PROX. (c) The same as (a) except for β_8 have the positive value. (d) The same as (b) except for β_8 have the positive value.

Fig.8 shows us the behavior of the effect of the deformation order β_8 on the radius of Coulomb barrier R_B as a function of θ_2 evaluated using DFM and PROX. DFM present a smooth relation for all the reactions. The curves of PROX shows abnormal behavior of the effect on the radius of Coulomb barrier for all range of mass number for the deformed nucleus.

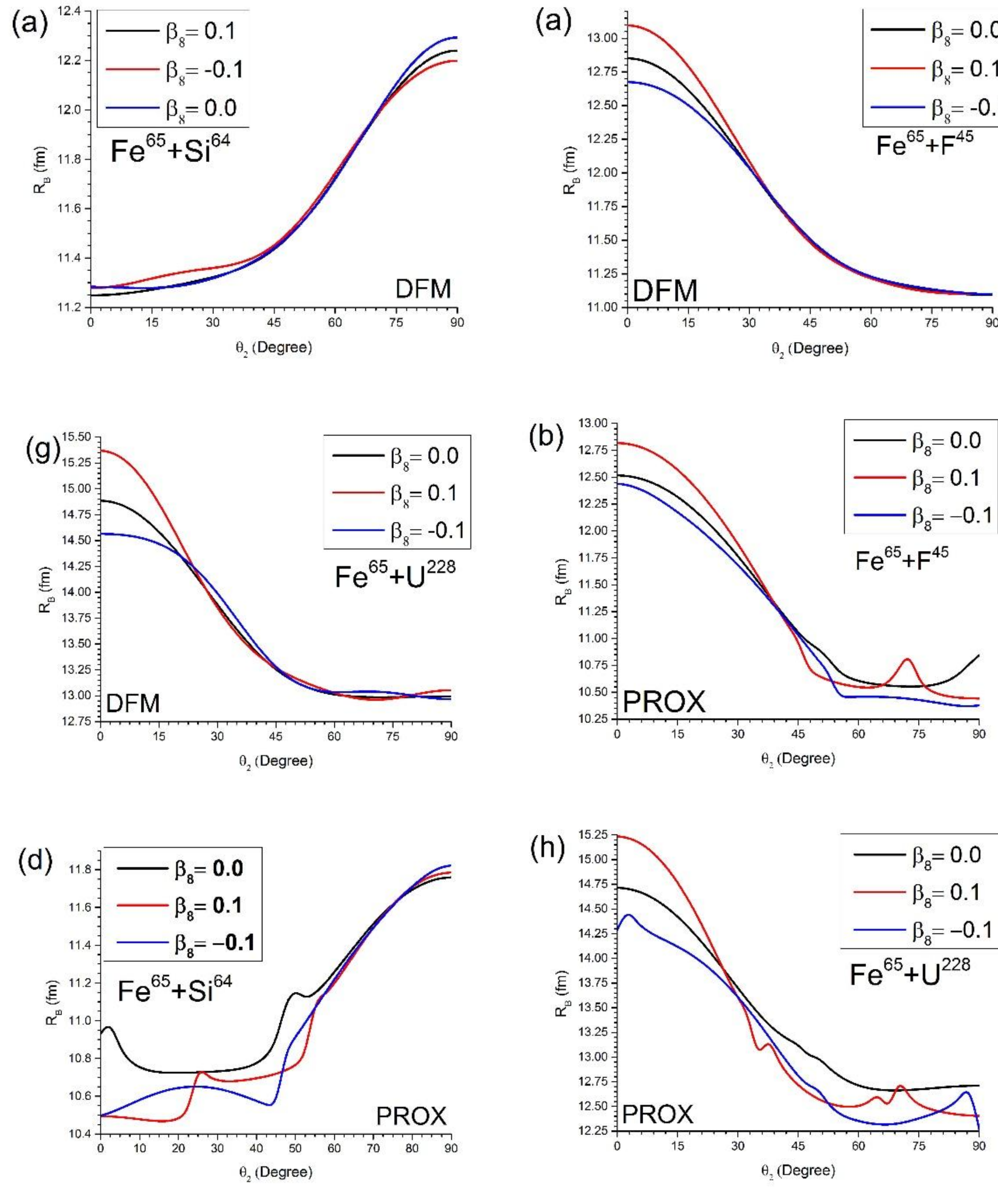

Figure 8 The radius of the Coulomb barrier, R_B, plotted as a function of the orientation angle θ_2 for $Fe^{65} + F^{45}$ interaction, in the frame work of DFM in Fig. a and proximity in Fig. b. Figures c & d are the same as a & b except for the reaction $Fe^{65} + Si^{64}$. Figures e & f are the same as a & b except for the reaction $Fe^{65} + Ba^{159}$. Figures g & h are the same as a & b except for the reaction $Fe^{65} + U^{228}$. We employed the deformation parameters of the deformed nuclei written on the graphs using negative, positive and zero value of β_8.

Table 4 The values of the fusion barrier parameters R_B and V_B and their relative variation R_r and V_r for $Fe^{65} + F^{45}$ & $Fe^{65} + Si^{64}$ interaction systems, using DFM and PROX

Reaction	θ_2	R_B	R_r	V_B	V_r	R_B	R_r	V_B	V_r	β_6
	(Deg)	*(fm)*		*(Mev)*		*(fm)*		*(Mev)*		
		DFM	DFM	DFM	DFM	PROX	PROX	PROX	PROX	
$Fe^{65} + F^{45}$	0	13.10	1.91	24.78	-1.80	12.82	2.41	25.12	-2.26	0.1
	10	12.96	1.67	25.02	-1.59	12.71	2.25	25.31	-2.11	
	20	12.58	1.05	25.71	-0.97	12.38	1.77	25.89	-1.67	
	30	12.09	0.38	26.65	-0.27	11.88	0.96	26.85	-0.93	
	40	11.65	0.01	27.48	0.03	11.27	-0.15	28.11	0.09	
	50	11.36	-0.02	27.96	-0.02	10.65	-2.32	29.57	2.09	
	60	11.22	0.01	28.16	-0.02	10.55	-0.53	29.74	0.51	
	70	11.14	-0.06	28.24	0.04	10.71	1.50	29.30	-1.11	
	80	11.10	-0.01	28.24	-0.04	10.48	-0.93	29.78	0.86	

	90	11.10	0.06	28.23	-0.12	10.44	-3.72	29.86	3.53	
	0	12.68	-1.37	25.59	1.39	12.44	-0.62	25.85	0.56	-0.1
	10	12.60	-1.14	25.71	1.14	12.30	-1.01	26.11	0.95	
	20	12.38	-0.58	26.10	0.54	12.03	-1.12	26.61	1.07	
	30	12.04	-0.04	26.71	-0.04	11.68	-0.70	27.28	0.68	
	40	11.67	0.19	27.41	-0.22	11.26	-0.19	28.14	0.21	
	50	11.38	0.16	27.93	-0.12	10.80	-0.98	29.16	0.68	
	60	11.23	0.12	28.14	-0.11	10.46	-1.38	29.97	1.28	
	70	11.16	0.15	28.19	-0.15	10.45	-1.01	29.90	0.90	
	80	11.12	0.11	28.23	-0.07	10.40	-1.68	29.98	1.54	
	90	11.10	0.04	28.26	0.00	10.38	-4.29	30.05	4.19	
$Fe^{65}+Si^{64}$	0	11.28	0.31	42.98	-0.44	10.49	-4.01	45.82	3.41	0.1
	10	11.28	0.17	43.03	-0.26	10.48	-2.54	45.94	2.00	
	20	11.28	-0.03	43.11	0.02	10.48	-2.27	46.13	2.10	
	30	11.32	-0.04	43.11	0.06	10.68	-0.45	45.44	0.44	
	40	11.39	0.03	43.01	-0.08	10.69	-0.73	45.48	0.56	
	50	11.51	0.01	42.76	-0.05	10.76	-3.60	45.38	3.12	
	60	11.72	-0.03	42.22	0.06	11.20	-0.53	43.88	0.50	
	70	11.98	0.08	41.44	-0.06	11.49	-0.16	42.91	0.12	
	80	12.21	0.32	40.76	-0.31	11.71	0.12	42.24	-0.16	
	90	12.29	0.44	40.50	-0.43	11.79	0.22	42.00	-0.26	
	0	11.28	0.26	43.12	-0.12	10.50	-3.99	45.99	3.80	-0.1
	10	11.30	0.34	43.04	-0.24	10.58	-1.59	45.62	1.29	
	20	11.33	0.43	42.93	-0.40	10.64	-0.74	45.39	0.45	
	30	11.36	0.33	42.95	-0.32	10.64	-0.85	45.49	0.54	
	40	11.40	0.16	42.99	-0.12	10.57	-1.84	45.91	1.52	
	50	11.53	0.14	42.74	-0.10	10.91	-2.26	44.79	1.78	
	60	11.74	0.16	42.12	-0.19	11.22	-0.34	43.78	0.27	
	70	11.98	0.03	41.44	-0.07	11.49	-0.17	42.92	0.15	
	80	12.14	-0.22	40.97	0.20	11.71	0.14	42.25	-0.12	
	90	12.20	-0.34	40.81	0.33	11.82	0.54	41.91	-0.49	

Table 5 The values of the fusion barrier parameters R_B and V_B and their relative variation R_r and V_r for $Fe^{65}+Ba^{159}$ & $Fe^{65}+U^{228}$ interaction systems, using DFM and PROX.

Reaction	θ_2	R_B	R_r	V_B	V_r	R_B	R_r	V_B	V_r	β_6
	(Deg)	(fm)		(Mev)		(fm)		(Mev)		
		DFM	DFM	DFM	DFM	PROX	PROX	PROX	PROX	
$Fe^{65}+Ba^{159}$	0	13.92	1.85	145.52	-2.02	13.62	1.41	147.53	-2.15	0.1
	10	13.81	1.25	146.50	-1.39	13.51	1.15	148.63	-1.83	
	20	13.57	0.09	148.76	-0.09	13.25	0.06	151.49	-0.44	
	30	13.34	-0.44	150.68	0.52	13.25	0.38	149.70	0.24	
	40	13.13	-0.08	151.90	0.07	12.73	-1.03	155.73	0.95	
	50	12.87	0.37	153.65	-0.45	12.46	-0.85	157.41	0.33	
	60	12.57	0.30	156.33	-0.31	12.13	-1.02	160.40	0.25	
	70	12.32	0.03	158.50	0.02	11.86	-2.47	163.93	1.76	
	80	12.23	0.11	158.95	-0.12	11.64	-2.45	164.92	1.60	
	90	12.22	0.28	158.74	-0.33	11.63	-1.78	164.30	0.64	
	0	13.56	-0.78	150.05	1.03	12.97	-3.44	156.26	3.63	-0.1
	10	13.60	-0.27	149.14	0.39	13.08	-2.73	153.78	2.40	
	20	13.64	0.61	147.97	-0.62	13.20	-0.97	151.62	0.42	
	30	13.51	0.87	148.55	-0.90	13.13	-0.02	151.61	-0.54	
	40	13.19	0.39	151.20	-0.39	12.85	0.03	153.93	-0.47	
	50	12.81	-0.11	154.60	0.17	12.47	-0.59	157.96	0.35	
	60	12.52	-0.07	156.92	0.06	12.10	0.10	161.67	0.18	
	70	12.34	0.17	158.07	-0.26	11.82	-2.72	163.33	1.67	
	80	12.23	0.08	158.96	-0.11	11.73	-1.73	164.27	0.90	
	90	12.18	-0.08	159.43	0.10	11.54	0.10	165.29	0.29	
$Fe^{65}+U^{228}$	0	15.37	3.25	216.88	-3.14	15.24	3.54	215.51	-3.99	0.1
	10	15.14	2.63	219.70	-2.63	15.03	3.27	218.30	-3.71	
	20	14.52	0.98	228.07	-1.05	14.42	1.96	226.69	-2.42	
	30	13.85	-0.23	238.19	0.40	13.60	-0.29	239.55	-0.16	
	40	13.40	-0.15	243.85	0.14	12.96	-0.90	249.82	1.13	
	50	13.17	0.28	246.01	-0.43	12.57	-2.91	252.72	1.15	
	60	13.03	0.11	247.63	-0.09	12.50	-2.02	254.52	0.74	
	70	12.96	-0.19	247.82	0.21	12.79	-1.69	252.14	0.85	
	80	13.01	0.12	246.18	-0.20	12.45	-1.63	253.14	0.81	
	90	13.06	0.46	245.17	-0.51	12.40	-2.38	252.12	0.48	
	0	14.57	-2.16	229.10	2.32	14.29	-2.88	232.30	3.49	-0.1

	10	14.53	-1.49	229.24	1.60	14.22	-2.50	232.31	2.92	
	20	14.37	-0.06	230.64	0.07	13.99	-1.84	233.62	1.51	
	30	13.99	0.80	235.06	-0.92	13.61	-0.80	237.80	-0.06	
	40	13.49	0.48	242.24	-0.52	13.08	-0.89	245.64	-0.35	
	50	13.13	0.00	247.33	0.10	12.68	-2.35	254.58	1.41	
	60	13.03	0.17	247.30	-0.22	12.35	-2.90	255.13	1.39	
	70	13.04	0.42	246.12	-0.48	12.33	-2.74	253.32	0.47	
	80	13.00	0.09	246.48	-0.08	12.45	-2.13	253.44	0.69	
	90	12.97	-0.22	247.03	0.25	12.27	0.12	257.61	0.44	

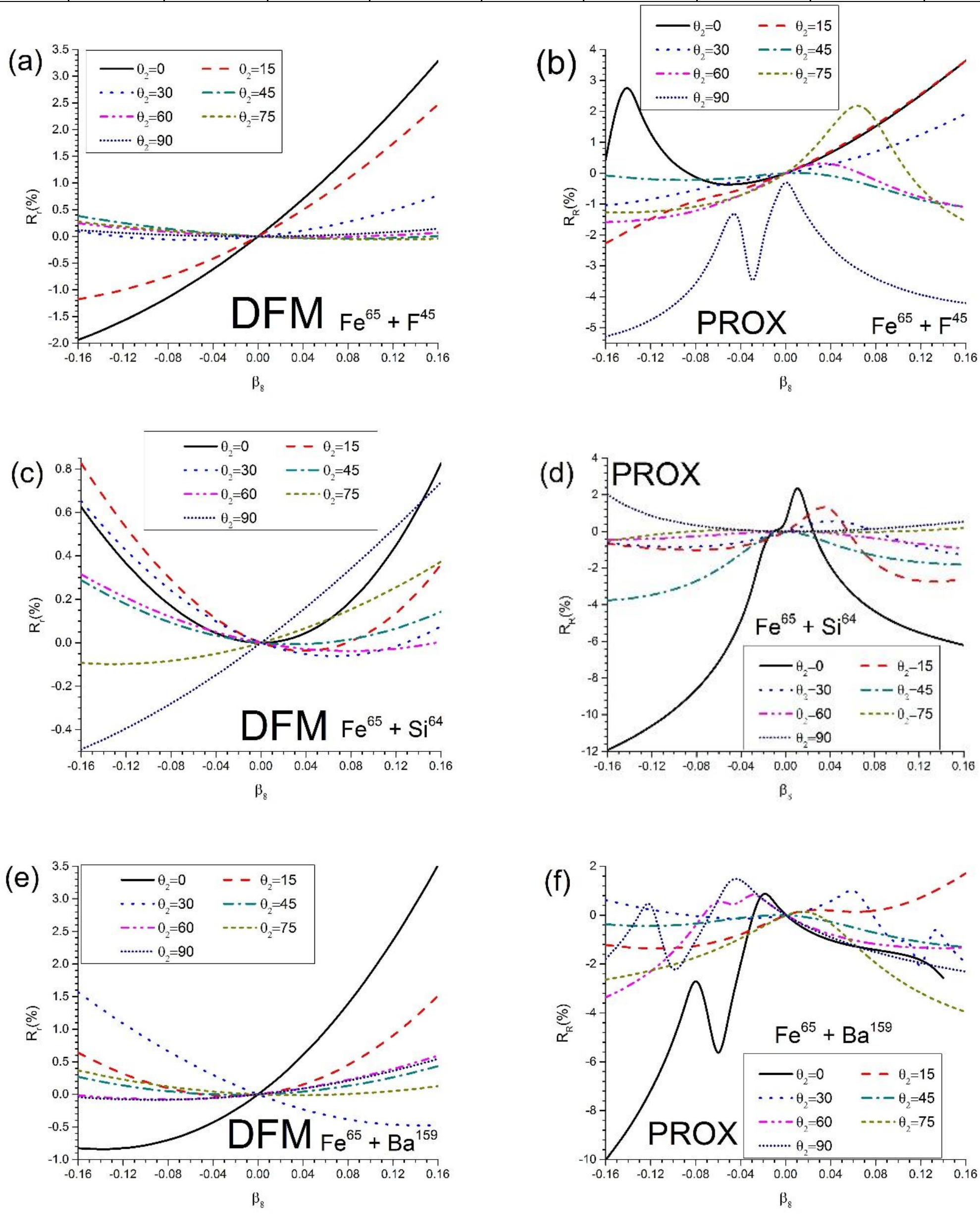

Figure 9 (a) The relative variation of the radius of Coulomb barrier, R_B, plotted as a function of the deformation order β_8 for $Fe^{65} + F^{45}$ interaction at its data in Table1 in the frame work of DFM. (b) The same as (a) except for using PROX. (c) The same as (a) except for $Fe^{65} + Si^{64}$ interaction. (d) The same as (b) except for $Fe^{65} + Si^{64}$ interaction.(e) The same as (a) except for $Fe^{65} + Ba^{159}$ interaction. (f) The same as (b) except for $Fe^{65} + Ba^{159}$ interaction.

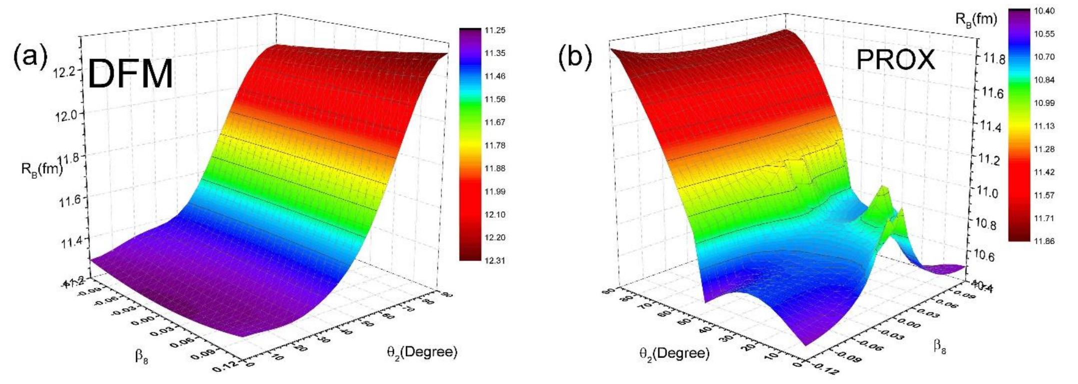

Figure 10 (a) The radius of the Coulomb barrier, R_B, plotted as a function of the orientation angle θ_2 and the deformation order β_6 for $Fe^{65}+Si^{64}$ interaction, using DFM calculation method. (b) The same as (a) except for using PROX calculation method.

Fig.9 presents the relative variation of the radius of Coulomb barrier R_r calculated by (eq.24) as a function of the deformation parameter β_8 at different orientation angles for the $Fe^{65}+F^{45}$, $Fe^{65}+Si^{64}$ & $Fe^{65}+Ba^{159}$ interaction systems. As shown in Figs. a, c and e DFM gives a smooth behavior for the relative variation of the radius of the Coulomb barrier with changing the deformation order β_8 . On the other hand, PROX introduces more irregularities in the curves representing the relation between the relative variation of the radius of Coulomb barrier R_r and the deformation order parameter β_8. PROX gives a peaks in the curves for the angles 0^o , 75^o & 60^o. As can be seen from the figure angle 15^o gives increasing relation for $Fe^{65}+F^{45}$ reaction, a peak for $Fe^{65}+Si^{64}$ reaction and small oscillation in an increasing relation for $Fe^{65}+Ba^{159}$ reaction. Fig.10 gives us more deep view on the behavior deformation order derived from different calculation method. It also confirm on the smoothness of DFM derived behavior and the strong abnormal behavior of proximity approach.

Tab.4 show quantitative behaviors of the fusion barrier parameters R_B and V_B and their relative variation R_r and V_r for $Fe^{65}+F^{45}$ and $Fe^{65}+Si^{64}$ interaction system, using DFM and PROX for orientation angles from 0^o to 90^o at the positive and negative values of β_8 of the deformed target nuclei. Tab.5 is the same as Tab.4 except for the reaction systems $Fe^{65}+Ba^{159}$ and $Fe^{65}+U^{228}$. It is obvious that Tables 4-5 ensure and enhance the failure of PROX to reproduce smooth and physical behaviors of dependence of the fusion barrier on the symmetry axis orientation and the deformation order β_8 of the target nucleus. For instance from Tab.5 for U^{228} at $\theta_2=90^o$ PROX produces larger value for the fusion barrier height V_B than its value from DFM by the difference 10.58 MeV. This larger difference in V_B is very effective in calculating the fusion cross sections.

IV. Conclusion

In summary we studied the effect of higher deformation orders on the fusion barrier parameter for spherical - deformed interactions. RB was computed using double folding method and a simple model based on version of PROX for nuclear part combined with Denisov's formula for the Coulomb part. In first place we found that proximity approach effects calculated for deformation order β6 is close to that of effect calculated by DFM for heavier nuclei, especially for orientation angles less than 55o. The relative variations of the radius of Coulomb barrier for DFM shows a behavior similar to the spherical harmonic Y60 function for deformation order β6 and similar to the spherical harmonic Y80 function for deformation order β8. Secondly PROX gives abnormal behavior which arose from the irregularities added to the nucleus and the concave regions in the nucleus surface due to the presents of the deformation orders β6 & β8. The relative variation of the radius of Coulomb barrier of adding deformation orders β6 or β8 is affected by the values other deformation parameters for both methods.

References

[1]. A.J.Baltz, B.F.Bayman. Proximity potential for heavy ion reactions on deformed nuclei. Physical Review C, 26:1969-1983, 1982.

[2]. Deepika Jain, Raj Kumar, Mano jK.Sharma. Effectof deformation and orientationon interaction barrier and fusion cross-sections using various proximity potentials. Nuclear Physics A, 915:106-124, 2013.

[3]. Deepika Jain, Raj Kumar, Manoj K.Sharma. Effect of deformation and orientation on interaction barrier and fusion cross-sections using various proximity potentials. Nuclear Physics A, 915:106-124, 2013.

[4]. G.R. Satchler, W.G. Love. Folding Model Potentials from Realistic Interactions for Heavy-ion Scattering. Physics Reports, 55:183-254, 1979.

[5]. I. I. Gontchar, M. V. Chushnyakova. The M3Y Double Folding Dissipative Model in Agreement with Precise Fusion Cross Sections. Journal of Modern Physics, 4:1-4, 2013.

[6]. Ishwar Dutt, Rajeev K. Puri. Analytical parametrization of fusion barriers using proximity potentials. Physical Review C, 81:064608, 2010.

[7]. Ishwar Dutt, Rajeev K. Puri. Role of surface energy coefficients and nuclear surface diffuseness in the fusion of heavy-ions. Physical Review C, 81:047601, 2010.

[8]. J. Blocki, J. Randrup, W. J. Swqtecki, C. F. Tsang. Proximity Forces. Annals of Physics, 105:427-462, 1977.

[9]. L. C. Chamon, B. V. Carlson, L. R. Gasques, D. Pereira, C. De Conti, M. A. G. Alvarez, M. S. Hussein, M. A. Candido Ribeiro, E. S. Rossi, Jr., C. P. Silva1. Toward a global description of the nucleus-nucleus interaction. Physical Review C, 66:014610, 2002.

[10]. M. Balasubramaniam, N. Arunachalam. Proton and radioactivity of spherical proton emitters. Physical Review C, 71:014603, 2005.

[11]. M. Ismail, A. Adel. Azimuthal angle dependence of the Coulomb barrier parameters for the interaction between two deformed nuclei. Physical Review C, 84:034610, 2011.

[12]. M. Ismail, A.Y. Ellithi, M.M. Botros, A.F. Abdel Reheem. Fusion barrier parameters for a spherically deformed pair of nuclei. Canadian Journal of Physics, 92:1411-1418, 2014.

[13]. M. Ismail, I.A.M. Abdul-Magead. Comparative study of Coulomb barrier parameters for deformed nuclei using double-folding model and proximity approach. Nuclear Physics A, 888:34-43, 2012.

[14]. M. Ismail, I.A.M. Abdul-Magead. Comparison between different proximity potentials and the double-folding model for spherical-deformed interacting nuclei. Canadian Journal of Physics, 94:102-111, 2015.

[15]. M. Ismail, I.A.M. Abdul-Magead. Examples of the failure of proximity approach when the nuclear surface is irregular or has concave regions. Nuclear Physics A, 922:168-179, 2013.

[16]. M. Ismail, W.M. Seif, H. El-Gebaly. On the Coulomb interaction between spherical and deformed nuclei. Physics Letters B, 563:53-60, 2003.

[17]. M. Ismail, W.M. Seif, M.M. Botros. Effect of octupole and higher deformations on Coulomb barrier. Nuclear Physics A, 828:333-347, 2009.

[18]. M. Seiwert, W. Greiner, V. Oberacker, M. J. Rhoades-Brown. Test of the proximity theorem for deformed nuclei. Physical Review C, 29:477-485, 1984.

[19]. Mark J. Rhoades-Brown, Volker E. Oberacker, Martin Seiwert, Walter Greiner. Potential Pockets in the 238 U+ 238 U System and Their Possible Consequences. Z. Phys. A - Atoms and Nuclei, 310:287-294, 1983.

[20]. Monika Manhas, Raj K. Gupta. Proximity potential for deformed, oriented nuclei: "Gentle" fusion and "hugging" fusion. Physical Review C, 72:024606, 2005.

[21]. O.N. Ghodsi. Simplification of Double Folding Model Calculations in Study of Interaction Between Two Deformed Nuclei. Communications in Theoretical Physics, 53(6):1140-1144, 2009.

[22]. P. Moller, A. J. Sierk, R. Bengtsson, T. Ichikawa, H. Sagawa. Nuclear shape isomers. Atomic Data and Nuclear Data Tables, 98:149-300, 2012.

[23]. Raj K Gupta, Dalip Singh, RajKumar, Walter Greiner. Universal functions of nuclear proximity potential for Skyrme nucleus-nucleus interaction in a semiclassical approach. Journal of Physics G: Nuclear Physics, 36:075104, 2009.

[24]. Raj K. Gupta, Monika Manhas, G. Munzenberg, Walter Greiner. Theory of the compactness of the hot fusion reaction 48Ca+244Pu—>292114. Physical Review C, 72:014607, 2005.

[25]. Raj K. Gupta, Narinder Singh, Monika Manhas. Generalized proximity potential for deformed, oriented nuclei. Physical Review C, 70:034608, 2004.

[26]. Rajeev K. Puri, Raj K. Gupta. Fusion barriers using the energy-density formalism: Simple analytical formula and the calculation of fusion cross sections. Physical Review C, 45(4):1837-1849, 1992.

[27]. V. Yu. Denisov, N. A. Pilipenko. Interaction of two deformed, arbitrarily oriented nuclei. Physical Review C, 76:014602, 2007.

[28]. W. D. Myers, W. J. Swiatecki. Nucleus-nucleus proximity potential and superheavy nuclei. Physical Review C, 62:044610, 2000.

[29]. Zhang Gao-Long, Liu Hao, Le Xiao-Yun. Nucleon-nucleon interactions in the double folding model for fusion reactions. Chinese Physi